CHINESE JOURNAL OF PHYSICS VOL. 32, NO. 2 APRIL 1994

Effects of Boson-Fermion Mixtures in Pt Isotopes

H. C. Chiang and S. T. Hsieh
Department of Physics, National Tsing Hua University, Hsinchu, Taiwan 300, R.O.C.

D. S. Chuu
Department of Electrophysics, National Chiao-Tung University, Hsinchu, Taiwan 300, R.O.C.

(Received December 7, 1993)

The Pt isotopes are studied in the boson-plus-fermion-pair model. The $1i_{13/2}$, $1h_{9/2}$ and $2f_{5/2}$ fermion orbitals are included in the model space. Isotopes quite near to the closed shells are included in the calculation. It was found that significant influences to the energy levels could be produced by the small mixtures from the fermion-pair configurations. The energy spectra and moment of inertia backbendings can he reproduced quite well. The calculated $B(E2)$ values show prominent dips at the onsets of different, fermion-pair configurations.

PACS. 21.60.Fw – Models based on group theory.
PACS. 27.70.+q – $150 \leq A \leq 189$.
PACS. 27.80.+w – $190 \leq A \leq 213$.

I. INTRODUCTION

The nuclei in the deformed and transitional region show regular nuclear collective properties. The algebraic collective model, the interacting boson approximation (IBA) [1-4], has been successfully applied to correlate these properties. The model is particularly successful for the low energy states. The model was extended to include the single-particle degrees of freedom. The estended model known as boson-plus-fermion model which includes fermion pairs as well as bosons has been applied mainly to correlate high spin anomalies related to the particle alignments.

The high-spin states of the even mass Pt isotopes show quite interesting properties [5-8]. The energy level spacings for the yrast states usually reduce considerably between the 10^+ and 12^+ states. The $B(E2)$ values of ^{184}Pt show a rather prominent decrease at the 10^+ state [7]. These high spin anomalies for $^{182-192}$Pt were analyzed in the boson-plus-fermion model by including a fermion pair distributed in $1i_{13/2}$ and $1h_{9/2}$ orbitals [9].

The model was quite successful in correlating the high spin anomalies of
It is generally believed that the single-particle degrees of freedom will be
in the neighborhoods of closed shells. Therefore: it will be interesting

[10-14].

Therefore, the purpose of this work is twofold. First, we wish to study the importance of the single-particle degrees of freedom by going closer to the closed shells and by including more fermion orbits. Second, we wish to present a systematical study for the Pt isotopes by including the most up to date experimental data.

II. MODEL

In the model space, both the pure boson and the boson plus fermion pair basis states are included. Thus the basis states stand the form

$$|n_s n_d \nu I\rangle \oplus |\tilde{n}_s \tilde{n}_d \tilde{\nu} L, (j_1 j_2) J; I\rangle \,. \tag{1}$$

Here $n_s(\tilde{n}_s)$ $n_d(\tilde{n}_d)$ are the number of s- and d-bosons respectively. The total number $N_B = n_s + n_d =$ ii, $+ \tilde{n}_d + 1$. The ν (Y) and L mean the additional quantum numbers which are needed to specify the boson part of states. In this work for $^{186-200}$Pt, N_B (number of boson holes) takes the values from 11 to 4 basing on the closed shell at $N = 126$ and $Z = 82$. The fermion single-particle angular momenta are denoted as j_1, j_2 and J is the total angular momentum of the fermion pair. In this work the $1i_{13/2}, 1h_{9/2}$ and $2f_{5/2}$ orbitals are included. Since we consider only positive parity states, the fermion pair states include $(i_{13/2})^2, (h_{9/2})^2, (f_{5/2})^2$ and $(h_{9/2} f_{5/2})$ configurations.

The Hamiltonian takes the form [15]

$$H = H_B + H_F + V_{BF} \,. \tag{2}$$

Here H_B is the boson part of Hamiltonian which takes the multipole expansion form [16]

$$H_B = \epsilon_d n_d + a_1 p^\dagger \cdot p + a_2 L \cdot L + a_3 Q \cdot Q \,, \tag{3}$$

where ϵ_d is the single-d boson energy and a_1, a_2 and a_3 are the strength parameters for pairing, angular momentum and quadrupole interactions respectively. H_F is the fermion part of Hamiltonian which includes the one-body and two-body fermion energies.

$$H_f = \sum_j \epsilon_j n_j \; \mathbf{t} \; \frac{1}{2} \sum_{J_{j_1 j_2 j_3 j_4}} V_0 \sqrt{2J+1} \, [(a^\dagger_{j_1} \times a^\dagger_{j_2})^{(J)} \times (\tilde{a}_{j_3} \times \tilde{a}_{j_4})^{(J)}]^{(0)} \,, \tag{4}$$

where ϵ_j is the fermion energy in the j single-particle orbit. In calculating the fermion two body interactions the Yukawa potential with the Rosenfeld mixture is used. The harmonic

oscillator wave functioins are used with the oscillator constant (0.96) $.(A^{-1/3}).10^{-22}\,\mathrm{sec}^{-1}$ where $A = 190$. The overall strength normalization is fixed by choosing V_0 as 50 MeV. V_{BF} is the boson-fermion interaction which takes the form

$$V_{BF} = Q \cdot \left\{ \sum_{j_1 j_2} (a^{\dagger}_{j_1} \times \tilde{a}_{j_2})^{(2)} + \sum_{j_1 j_2 j_3 j_4} [(a^{\dagger}_{j_1} \times a^{\dagger}_{j_2})^{(4)} \times \tilde{d} - d^{\dagger} \times (\tilde{a}_{j_3} \times \tilde{a}_{j_4})^{(4)}]^{(2)} \right\} \tag{5}$$

and

$$Q = (d^{\dagger} \times \tilde{s} + s \times \tilde{d})^{(2)} - \frac{\sqrt{7}}{2} (d^{\dagger} \times \tilde{d})^{(2)} . \tag{6}$$

The whole Hamiltonian is then diagonalized in the selected model space and the interaction parameters are determined by least-squares fittings to the esperimental energy levels of $^{186-200}$Pt. The resulting wave functions are used to calculate the $B(E2)$ values.

III. RESULTS

In determining the interaction parameters we tried to unify the parameters corresponding to the isotope chain as much as possible. The parameters are varied smoothly when this is needed in reproducing good theory-esperiment energy levels agreements. The adopted interaction parameters are listed in Table I. The angular momentum interaction

TABLE I. Adopted interaction parameters in MeV.

	ϵ_d	a_1	a_3	$\epsilon_{11/2}$	$\epsilon_{9/2}$
^{186}Pt	0.3640	0.0400	-0.0064	1.5741	0.7992
^{188}Pt	0.4560	0.0330	-0.0030	1.4277	1.1809
^{190}Pt	0.5042	0.0690	-0.0005	1.4457	1.2806
^{192}Pt	0.5608	0.1069	-0.0009	1.4090	1.6000
^{194}Pt	0.6052	0.1900	-0.0011	1.5149	1.5434
^{196}Pt	0.5909	0.2158	-0.0021	1.5588	1.4593
^{198}Pt	0.5374	0.1400	0.0160	1.3510	1.5000
^{200}Pt	0.5648	0.2.500	0.0084	1.7297	1.5750

parameter a_2, the boson-fermion interaction parameters α, β, and the single-fermion energy $\epsilon_{5/2}$ can be unified for the isotope chain. The values are a_2 = 0.01 MeV, α = 0.09 MeV, β = 0.02 MeV and $\epsilon_{5/2}$= 1.70 MeV. For the smaller mass isotopes such as $^{186-188}$Pt the single d-boson energies are smaller as compared with the corresponding values for the other isotopes. This is consistent with the well-known O(G) to $SU(3)$ transition tendency for the Pt isotopes from ^{196}Pt to ^{186}Pt[17]. Other interaction parameters usually vary quite smoothly versus the change of masses.

The energy levels can be reproduced quite well in general. As illustrations, we present the calculated and experimental energy levels for $^{198-200}$Pt, $^{192-194}$Pt and ^{186}Pt in Figs. 1-3. The calculated energy levels for the other nuclei in this isotope chain show similar theory-experiment agreements. For the high mass isotopes $^{198-200}$Pt, the $0_1^+, 2_1^+, 2_2^+$ energy level sequence for the first three energy states which appears usually in the limit of O(G) symmetry can be reproduced. Going to the lighter mass isotopes the energies of the first 2^+ states decrease and the rotational features of the yrast states become more prominent.. All of these features can be reproduced. In general, the theory-experiment agreements for the even-J state are quite good except for the excited 0^+ states. Also, on average the agreements for the odd-J states are not so good as those for the even-J states. For the $^{198-200}$Pt isotopes, no high-spin states have been observed. When the mass number decreases, the energy level density become more dense and more high spin states appear.

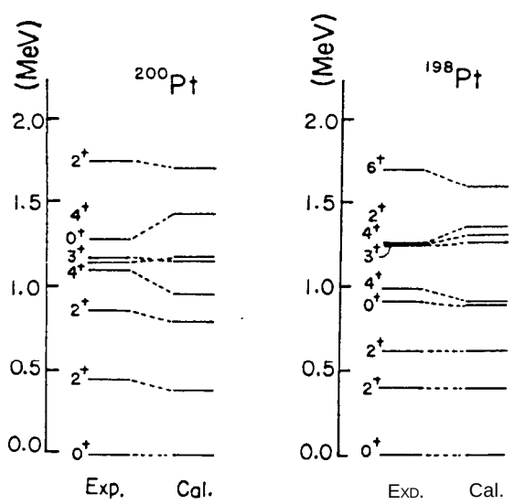

FIG. 1. Calculated and experimental energy levels for ^{198}Pt and ^{200}Pt. The experimental data are adopted from Reis. 11 (^{198}Pt) and 18, 19 (^{200}Pt).

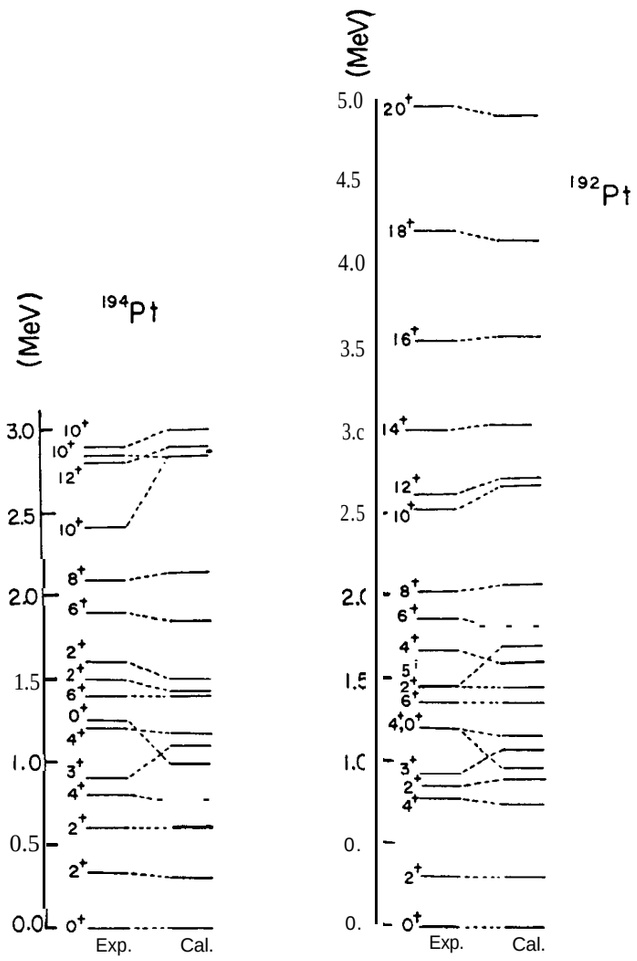

FIG. 2. Calculated and experimental energy levels for ^{192}Pt. The experimental data are adopted from Ref. 20.

For ^{186}Pt state of spin up to 26 and for ^{192}Pt up to 20 have been observed [12,16]. The prominent narrow energy spacing between the 12_1^+ and 10_1^+ of ^{192}Pt state can be reproduced. The high spin states of ^{186}Pt are quite numerous and can be reproduced quite nicely.

The high spin anomalies can be also manifested in the sensitive $2\mathcal{J}/\hbar^2$ versus $(\hbar\omega)^2$ plot. In general the plots obtained in this work are similar to those of Ref. 9. In Figs. 4, 5 we present only the plots of $^{186-188}$Pt which are more complete than those of Ref. 9 due to the availability of more experimental data. Note that the corresponding plot of ^{186}Pt of

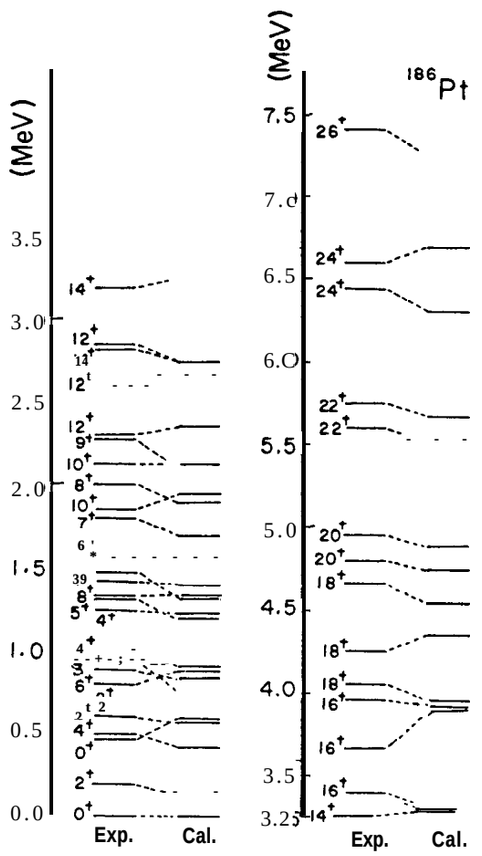

FIG. 3. Calculated and experimental energy levels for ^{186}Pt. The experimental data are adopted from Ref. 12.

Ref. 9 does not show any backbending due to the lackness of high spin state data at the time when the calculation was performed. An analysis of the wave functions indicate that both $(i_{13/2})^2$ and $(h_{9/2})^2$ alignments happen in the high spin region. In Table II the dominant configurations for the high spin states of ^{186}Pt are listed for reference. Apparently the $f_{5/2}$ orbital does not have contributions to the high spin states. In general, the $f_{5/2}$ orbital is relatively much less important than the $i_{13/2}$ and $h_{9/2}$ orbitals. It was found that only some low-lying 0^+ and 2^+ states have significant contribution from the $f_{5/2}$ orbital. To be more specific, only the 8_2^+ state of ^{188}Pt, the 0_2^+ states of ^{190}Pt and ^{198}Pt, the 2_3^+ states of ^{194}Pt, ^{196}Pt, ^{198}Pt, ^{200}Pt and the 2_4^+ state of ^{192}Pt have more than 5 % of contributions of configurations involving the $f_{5/2}$ orbital. In general, it was found that the fermion-pair

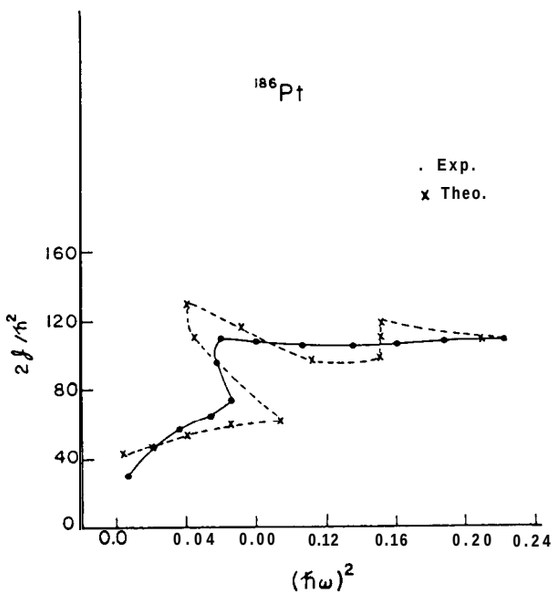

FIG. 4. Backbending plot for ^{186}Pt. The experimental data are adopted from Ref. 12.

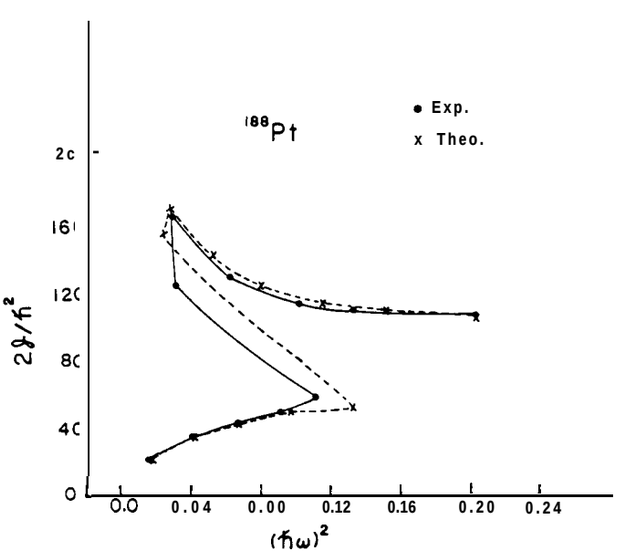

FIG. 5. Backbending plot for ^{188}Pt. The experimental data are adopted from Ref. 13.

TABLE II. The wave function intensity distributions for the high spin states of ^{186}Pt.

	Pure Boson	Boson plus $(i_{13/2})^2$	Boson plus $(h_{9/2})^2$	Boson plus $(f_{5/2})^2$	Boson plus $(f_{5/2}h_{9/2})$
14_1^+	0.000	0.003	0.997	0.000	0.000
14_2^+	0.000	0.008	0.991	0.000	0.001
14_3^+	0.001	0.003	0.995	0.000	0.001
16_1^+	0.000	0.003	0.997	0.000	0.000
16_2^+	0.000	0.006	0.994	0.000	0.000
16;	0.000	0.663	0.337	0.000	0.000
18_1^+	0.000	0.003	0.997	0.000	0.000
18_2^+	0.000	1.000	0.000	0.000	0.000
18;	0.000	0.003	0.997	0.000	0.000
20_1^+	0.000	0.003	0.997	0.000	0.000
20_2^+	0.000	1.000	0.000	0.000	0.000
22_1^+	0.000	1.000	0.000	0.000	0.000
22_2^+	0.000	0.003	0.997	0.000	0.000
24_1^+	0.000	1.000	0.000	0.000	0.000
24_2^+	0.000	0.003	0.997	0.000	0.000
26_1^+	0.000	1.000	0.000	0.000	0.000

configurations were important for higher states for a specific spin I. To be more specific, the $0_2^+, 2_3^+, 2_4^+, 4_3^+, 6_3^+$ and 8_2^+ states are usually dominated by the fermion-pair plus boson configurations. In Table III, the wave function intensities of these states are shown for reference. The contribution of the fermion-pair configurations are more important than the appearance in the wave functions intensities. Sometimes, the small contribution of the fermion-pair configurations can produce quite significant influence to the energy eigenvalues. This means that if the small contributions are removed by removing a single-particle orbit, rather drastical change of energy eigenvalues may be produced. As an example, if we remove the $h_{9/2}$ single-particle orbit, many states will have quite different energy values although the wave function intensity distributions are quite similar. In Table IV we present the energy eigenvalues and wave function intensity distributions of such states for reference. From the table we see that even if the contribution of the $(h_{9/2})^2$ configuration are quite small, significant change of calculating result can be produced if the orbit is removed. The change can be reflected in quite different wave function intensity distributions in the other orbits (such as the 2_5^+ state of ^{188}Pt, 2_4^+ state of ^{190}Pt, 10_2^+ state of ^{194}Pt and 2_4^+ state of

TABLE III. The wave function intensity distributions for the low-spin states which have significant boson-plus-fermion-pair configurations.

		Pure Boson	Boson plus $(i_{13/2})$	Boson plus $(h_{9/2})^2$	Boson plus $(f_{5/2})^2$	Boson plus $(f_{5/2}h_{9/2})$
^{186}Pt	4_3^+	0.228	0.587	0.166	0.018	0.001
	6_3^+	0.001	0.217	0.760	0.023	0.000
^{188}Pt	2_4^+	0.134	0.346	0.481	0.037	0.003
^{190}Pt	0_2^+	0.000	0.440	0.510	0.050	0.000
	2_3^+	0.000	0.442	0.504	0.044	0.001
^{192}Pt	2_3^+	0.081	0.112	0.064	0.012	0.731
	2_4^+	0.234	0.457	0.252	0.050	0.007
^{194}Pt	2_3^+	0.000	0.520	0.415	0.065	0.000
	8_2^+	0.000	0.171	0.829	0.000	0.000
^{196}Pt	2_3^+	0.000	0.464	0.474	0.061	0.001
^{198}Pt	0_2^+	0.000	0.578	0.369	0.053	0.000
	2_3^+	0.000	0.432	0.485	0.055	0.027
^{200}Pt	2_3^+	0.000	0.423	0.487	0.083	0.007

^{196}Pt) or just a big change in the energy eigenvalues. In the later case, the wave function intensity distributions still remain quite similar when we remove the $h_{9/2}$ orbital. However, the removal of the small configurations from the $h_{9/2}$ orbital forced us to select configurations from other orbitals. The situation is that the next available eigenstate is much higher than the original one and we get a much higher calculated energy eigenvalue. Therefore, for these state the $h_{9/2}$ orbital is defintely needed even if it contributes little to the wave functions.

The wave functions can be further tested by the electromagnetic transition rates. In this work, we calculated the $B(E2)$ values of the yrast band states. In boson-plus-fermion model the electric quadrupole transition operator is given by

$$T^{(2)} = e_B Q + e_F \sum_{j_1 j_2} \Big[\alpha (a_{j_1}^\dagger \times \tilde{a}_{j_2})^{(2)} + \beta e_B \sum_{j_1 j_2 j_3 j_4} \Big[(a_{j_1}^\dagger \times a_{j_2}^\dagger)^{(4)} \times \tilde{d} - d^\dagger \times (\tilde{a}_{j_3} \times \tilde{a}_{j_4})^{(\cdot)} \Big]^{(2)} \Big], \tag{7}$$

where

$$Q = s \times \tilde{d} + d^\dagger \times s + \chi (d^\dagger \times \tilde{d})^{(2)} \tag{8}$$

TABLE IV. Comparison of the energy eigenvalues and the wave function intensity distributions for the cases the $h_{9/2}$ orbital is included (first line for each state) and removed (second line for each state).

Nucleus	State	E_{exp}	E_{Theo}	Boson	Boson plus $(i_{13/2})^2$	Boson plus $(h_{9/2})^2$	Boson plus $(f_{5/2})^2$	Boson plus $(f_{5/2}h_{9/2})$
^{186}Pt	2_1^+	0.192	0.136	**0.982**	0.002	0.008	0.003	0.005
	2_1^+	0.192	0.542	0.975	0.003	0.000	0.002	0.020
	2_2^+	0.607	0.564	0.983	0.002	0.007	0.002	0.006
	2_2^+	0.607	0.848	0.980	0.014	0.000	0.006	0.000
	2_3^+	0.798	0.872	0.976	0.004	0.015	0.002	0.003
	2_3^+	0.798	1.450	0.967	0.024	0.000	0.009	0.000
	4_1^+	0.490	0.429	0.981	0.002	0.009	0.002	0.006
	4_1^+	0.490	0.750	0.987	0.007	0.000	0.004	0.002
	8_1^+	1.342	1.341	0.931	0.004	0.039	0.006	0.017
	8_1^+	1.342	1.556	0.979	0.013	0.000	0.007	0.003
^{188}Pt	2_3^+	1.115	1.057	0.963	0.013	0.018	0.003	0.003
	2_3^+	1.115	1.530	0.974	0.016	0.000	0.010	0.000
	2_5^+	1.528	1.405	0.976	0.007	0.012	0.002	0.003
	2_5^+	1.528	3.825	0.162	0.474	0.000	0.364	0.000
^{190}Pt	2_4^+	1.395	1.332	0.988	0.003	0.004	0.002	0.003
	2_4^+	1.395	2.783	0.425	0.522	0.000	0.052	0.001
^{194}Pt	10_2^+	2.917	3.027	0.962	0.010	0.010	0.007	0.011
	10_2^+	2.917	3.201	0.121	0.878	0.000	0.001	0.000
^{196}Pt	2_4^+	1.604	1.635	0.997	0.001	0.001	0.001	0.000
	2_4^+	1.604	2.920	0.266	0.597	0.000	0.135	0.002

In the calculation it was found that the B(E2) values for the yrast states do not depend on the value of X sensitively. In reporting the B(E2) values, X = $\frac{-\sqrt{7}}{2}$ which corresponds to the $SU(3)$ value is selected. This unifies the Q operator of the $T^{(2)}$ and Hamiltonian. The effective charges e_F and e_B are chosen to be 0.37 and 0.15 of proton charge which are similar to the values chosen in the previous calculations. The calculated B(E2) values in general increase for low spin states region as I incleases then drop for higher spin region. Between I = 8 and I = 12, usually a quite sharp drop happens for the reason of the onset of the fermion-pair plus boson configurations. The experimental data for the B(E2) values of the Pt isotopes are quite meager. In Fig. 6 the calculated and experimental B(E2) values

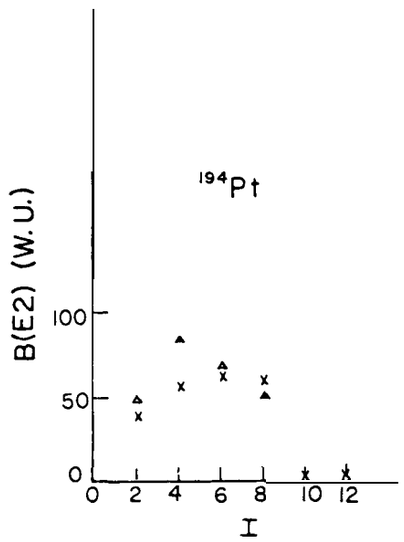

FIG. 6. Calculated (crosses x) and experimental (triangle A) $B(E2)$ values for ^{194}Pt. The experimental data are adopted from Ref. 21.

of the yrast band of ^{194}Pt are shown. It seems the relative higher experimental values of $I = 4$ state is not reproduced well. For the other states, the theory-experiment agreements are reasonably good. As illustrations we also present the calculated B(E2) values of ^{188}Pt and ^{190}Pt in Fig.7 .The general trend is to have a increase in *B(E2)* values in the low spin region and has a rather prominent dip at $I = 10$ where the boson and $(i_{13/2})^2$ fermion pair configurations become dominant. In Fig. S we also present the calculated B(E2) values for ^{186}Pt. No experimental data are available for comparison. It is interesting to see that there are two dips in the B(E2) values. The first one corresponds to the onset of $(h_{9/2})^2$ alignment and the second one corresponds to the $(i_{13/2})^2$ alignment. This double dip feature in B(E2) values can be used as a rather critical test of the validity of the calculation model.

IV. SUMMARY

In summary, the Pt isotopes are studied more extensively in the boson-plus-fermion model. As compared to the previous similar calculation, more single-particle orbitals are included in the fermion degrees of freedom. Also, more isotopes which lie closer to the doubly closed shell $N = 126$ and $Z = 82$ are included in the ca.lculatioin. It was found that significant influence to the energy levels can be produced by small mixtures from the

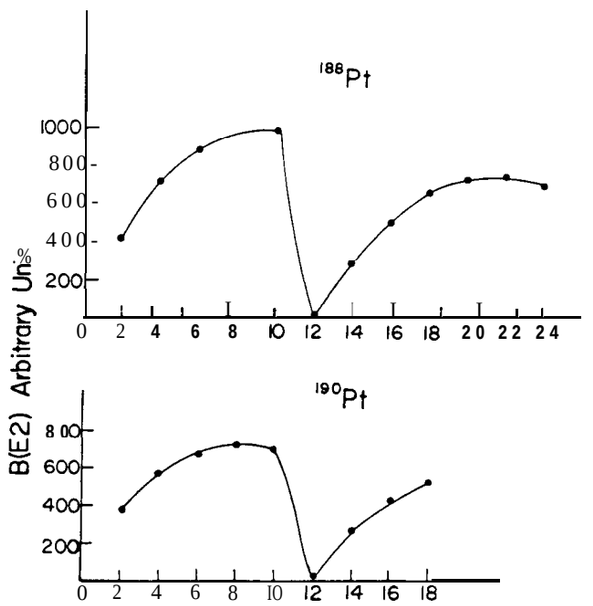

FIG. 7. Calculated $B(E2)$ values for ^{188}Pt and ^{190}Pt.

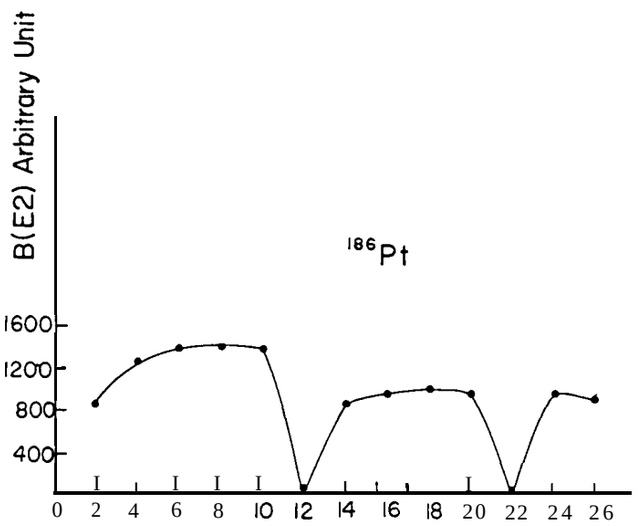

FIG. S. Calculated $B(E2)$ values for ^{186}Pt.

fermion-pair configurations. The backbending plots of the Pt isotopes can be reproduced. The calculated B(E2) values of the yrast states usually have a dip when the different fermion-pair configurations set in. Therefore, the calculated $B(E2)$ values of ^{186}Pt show two dips at $I = 10$ and 22. It can be used as a rather critical test of the validity of the model when the corresponding experimental data are available.

ACKNOWLEDGMENT

Work supported by the National Science Council, Republic of China with the grant No. NSC81-0208-M007-69.

REFERENCES

[1] A. Arima and F. Iachello, Ann. Phys. (N.Y.) 99, 253 (1976).

[2] A. Arima and F. Iachello, Ann. Phys. (N.Y.) 111, 201 (1978).

[3] A. Arima and F. Iachello, Ann. Phys. (N.Y.) **115,** 325 (1978).

[4] A. Arima and F. Iachello, Ann. Phys. (N.Y.) 123, 468 (1979).

[5] A. A. Raduta, C. Lima, and A. Faessler, Phys. Lett. **121B**, 1 (1953).

[6] G. D. Dracoulis et al., Jour. Phys. **G12**, 197 (1986).

[7] U. Gay et al., Phys. Lett. B180, 319 (1986).

[8] A. J. Larabee et al., Phys. Lett. **169B**, 21 (1986).

[9] D. S. Chuu, S. T. Hsieh, and H. C. Chiang, Phys. Rev. **C40**, 382 (1989).

[10] B. Singh, Nucl. Data Sheets 61, 243 (1990).

[11] Z. Chunmei, Nucl. Data Sheets 60, 527 (1990).

[12] G. Hebbinghaus, T. Kutsarova, W. Gast, A. Kramer-Flecken, R. M. Lieder, and W. Urban, Nucl. Phys. A514, 225 (1990).

[13] B. Singh, Nucl. Data Sheets, 59, 133 (1990).

[14] A. Mauthofer, I<. Stelzer, J. Idzko, Th. W. Elze, H. J. Wollersheim, H. Emling, P. Fuchs, E. Grosse, and D. Schwalm, Z. Phys. A336, 263 (1990).

[15] N. Yoshida and A. Arima, Phys. Lett. **164B**, 231 (1985).

[16] A. Arima and F. Iachello, Ann. Rev. Nucl. Part. Sci. 31, 7.5 (1981).

[17] R. T. Casten and J. A. Cizewski, Nucl. Phys. A309, 477 (1978).

[18] M. R. Schmorak, Nucl. Data Sheets **51,** 689(1987).

[19] S. W. Yates, E. M. Baum, E. A. Henry, L. G. Mann, N. Roy, A. Aprahamian, R. A. Meyer, and R. Estep, Phys. Rev. **C37**, 1889 (1988).

[20] v. s. Shirley and J. M. Dairiki, Nucl. Data Sheets 40, 425 (1983).

[21] B. Singh, Nucl. Data Sheets **56**, 75 (1989).